CALIBRATION OF A DISCRETE ELEMENT MODEL FOR SILAGE CORN STRAW CONSIDERING THE ENTIRE SHEARING PROCESS BASED ON BAYESIAN OPTIMIZATION

/

基于贝叶斯优化的青贮玉米秸秆全剪切历程离散元模型标定研究

Yunpeng YAN[1)], Shu ZHANG[1)], Xisheng ZHANG[2)], Ji ZHANG[1)], Qinglu YANG[1)], Fuyang TIAN[1)], Xiao SONG[3)], Zhanhua SONG *[1)]

[1)]College of Mechanical and Electronic Engineering, Shandong Agricultural University, Taian 271018 / China
[2)]JOTEC International Heavy Industry (Qingdao) Co., Ltd., Qingdao 266500 / China
[3)]Qingdao Zhongrui Weifei Marine Equipment Co., Ltd., Qingdao 266500 / China
Tel: +86-135 0548 4990; E-mail: songzh@sdau.edu.cn
DOI: https://doi.org/10.35633/inmateh-78-71

Keywords: *silage corn, discrete element method, entire shearing process, Bayesian optimization algorithm, parameter calibration, model validation*

ABSTRACT

The accuracy of discrete element simulations for silage corn stover is highly dependent on the precise calibration of model parameters. Addressing the relative scarcity of research on identifying DEM parameters for silage corn stover, this study constructs a simplified DEM model based on the Bonding constitutive model for granular materials. Parameter calibration is performed using experimental data on key physical and mechanical properties of the stover. Using the entire shear history stress-strain curve as the calibration benchmark, Gaussian process regression was introduced as a surrogate model. With mean squared error (MSE) as the objective function, a Bayesian optimization algorithm was employed to accurately identify the bonding parameters of the DEM model. The optimal parameter combination yielding the minimum MSE (MSE = 0.0072) was obtained: normal bonding stiffness, tangential bonding stiffness, normal strength, and shear strength were 5.12 × 10⁹ N/m³, 1.28 × 10⁸ N/m³, 1.60 × 10⁷ Pa, and 2.48 × 10⁶ Pa, respectively. To validate this parameter set, three-point bending tests were conducted and compared with simulation results. The bending stress-strain curves from the discrete element model closely matched experimental trends and peak characteristics, confirming the model's accuracy. The proposed Bayesian optimization-based parameter calibration method demonstrates high precision and efficiency. It provides reliable references for discrete element simulations of silage corn stalk processing and the design optimization of key components in harvesting machinery.

摘要

青贮玉米秸秆离散元仿真的准确性高度依赖于模型参数的精确标定，针对青贮玉米秸秆离散元参数的识别研究相对不足问题，本文基于颗粒粘结本构模型（Bonding）构建了一种青贮玉米秸秆离散元模型，并结合秸秆关键物理与力学特性试验开展了参数标定。以全剪切历程应力-应变曲线为标定基准，引入高斯过程回归作为代理模型，以均方误差（MSE）为目标函数，采用贝叶斯优化算法实现离散元模型粘结参数的准确识别。获得对应最小均方误差（MSE=0.0072）的最优参数组合：法向粘结刚度、切向粘结刚度、法向强度、剪切强度分别为5.12×109 N/m3、1.28×108 N/m3、1.60×107 Pa、2.48×106 Pa。为验证该参数组合的可靠性，进一步开展三点弯曲试验并与仿真结果进行对比。结果表明，离散元模型的弯曲应力-应变曲线与试验结果在变化趋势及峰值特征上吻合度较高，验证了模型的准确性。本研究提出的基于贝叶斯优化的参数标定方法精度和效率较高，可为青贮玉米秸秆加工过程的离散元仿真及收获机关键部件的设计优化提供可靠参考。

INTRODUCTION

In China, silage feeds account for 78.5% of beef cattle and sheep diets, with corn silage comprising 98% of this total (*Lu et al., 2021*). However, corn stalks used for silage are hard in texture and high in crude fiber content, resulting in poor palatability, low animal intake, and difficult digestion (*Guo et al., 2002*). Traditional physical crushing processes, such as chopping and shredding silage corn stalks, can enhance animals' digestibility of silage feed while increasing its nutritional value and utilization efficiency *(Liu et al., 2018*). Therefore, optimizing key components of silage stalk chopping and shredding equipment is crucial for improving feed quality. Traditional optimization methods (e.g., trial-and-error approaches) are costly and susceptible to experimental uncertainties (*Chen et al., 2018; Hou et al., 2023; Zhao et al., 2025)*.

The silage crushing process inherently constitutes a complex dynamic system involving interactions between numerous discrete bodies and mechanical structures (*Yu et al., 2005*). Consequently, the Discrete Element Method (DEM) can precisely simulate this process. To elucidate the coupled load-damage evolution mechanism between straw and roller teeth during shredding, establishing a constitutive model that characterizes their mechanical behavior is urgently needed.

The discrete element method (DEM) is a numerical simulation technique based on the assumption of discontinuity (*Wang et al., 2005*), first proposed by Chundall (1979) and applied to rock mechanics. In recent years, the application of DEM in agricultural engineering has become increasingly widespread *(Zhao et al., 2025*). *Liu et al. (2018)* developed a discrete element flexible straw model based on the Hertz-Mindlin theory with bonding to simulate wheat straw bending behavior. Parameter calibration was performed using three-point bending tests *(Zeng et al., 2024; Xing et al., 2017*) and Box-Behnken experiments. In 2022, *Guan et al. (2022)* established a flexible rapeseed stem model using the angle of repose as an evaluation metric, employing Plackett-Burman simulation verification and response surface analysis for parameter calibration. *Zhang et al. (2022)* established a discrete element model for water chestnut using maximum shear force as the evaluation metric, employing the steepest slope test and response surface analysis for parameter calibration. *He et al. (2025)* developed a discrete element soil interaction system using EDEM software. Researchers have also developed discrete element models for crops, including tobacco seeds *(Xie et al., 2025*), tea stems *(Du et al., 2025)*, and others *(Fu et al., 2025; Guo et al., 2025; LI et al., 2025; Liang et al., 2025; Ma et al., 2025; Xu et al., 2025*). *Shentu et al. (2023)* proposed an end-to-end machine learning framework and performed sensitivity analysis on each parameter. Calibrating accurate model parameters is a critical prerequisite for ensuring reliable simulation results and guiding engineering practice (*Liu et al., 2023*)

Existing parameter calibration for silage corn stalk discrete element models primarily relies on characteristic values such as peak force from compression or shear tests, failing to account for the stress-strain evolution throughout the stalk's failure process. However, the stress conditions during silage corn processing are equally important. To address this limitation, this study proposes using the entire shear history stress-strain curve as the calibration benchmark. By employing Bayesian optimization methods to calibrate cohesion parameters, a simplified discrete element model for silage corn stalks was established. This model comprehensively reflects the mechanical response during stalk failure, enhancing simulation efficiency while maintaining accuracy. The calibrated parameters were then validated through three-point bending tests on silage corn stalks.

MATERIALS AND METHODS

Collection of Corn Stalk Samples

This study utilized corn stalks from Shandong Agricultural University's experimental fields, employing the Denghai 605 corn variety. After corn plants reached target physiological maturity, 50 healthy plants with consistent growth and free of pests or diseases were randomly selected using the “S”-shaped layout method within the experimental field. For each corn stalk, after removing the root and cob, the section bearing the cob, along with the two adjacent sections above and below it, was designated as the middle section. The entire stalk was divided into three sections: upper, middle, and lower. After pruning, each section was immediately placed into separate sealed bags to prevent moisture loss.

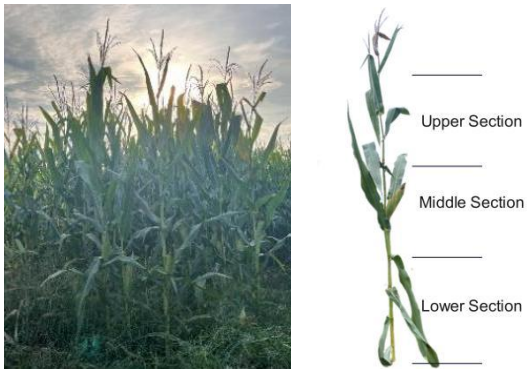

Fig. 1 - Maize plant

The physical and mechanical parameters measured for corn stover include moisture content, density, diameter, friction coefficient, and elastic modulus.

Moisture content significantly affects the mechanical properties of corn stover and was determined using the drying method, as shown in Figure 2. The physical and mechanical parameters of corn stover measured in the experiment are listed in Table 1.

Fig. 2 - Moisture content test

The elastic modulus of corn stalks was determined through axial compression testing, as shown in Figure 3a. Linear fitting was performed on the elastic deformation phase of the load-displacement curve to obtain the slope k. The formula for calculating the elastic modulus is:

$$E_c = \frac{\sigma_c}{\varepsilon_c} = \frac{F_c L_0}{S_c \Delta L} = \frac{4kL_0}{\pi d^2} \quad (1)$$

where:

σ_c is the compressive stress, MPa;

F_c is the axial force, N;

S_c is the cross-sectional area of the straw compression specimen, mm^2;

E_c is the compressive modulus of elasticity, MPa;

ε_c is the strain of the straw specimen;

d is the straw diameter, mm.

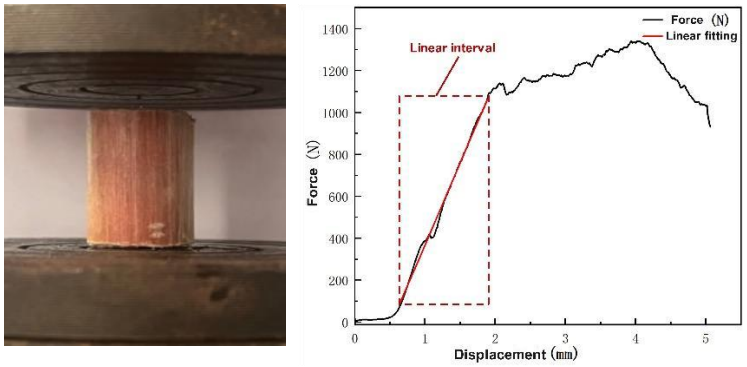

a-Compression test

b-Linear Fitting of Compression Test Load-Displacement Curve

Fig. 3 - Axial compression test

Calculations yielded an average elastic modulus of 95.94 MPa for corn stalks, with a standard deviation of 5.68.

Table 1

Measurement results of silage corn stalk parameters

Straw section	Upper Section	Central Region	Lower section
Average diameter (mm)	7.27	12.87	15.21
Average moisture content (%)	70.31	65.85	67.09
Density (kg/m3)		88	
Modulus of elasticity (MPa)		95.94	
Poisson ratio		0.35 (*Liu et al., 2023*)	

The coefficient of friction was measured using a friction coefficient tester, as shown in Figure 4. Three replicate tests were conducted, with the results presented in Table 2.

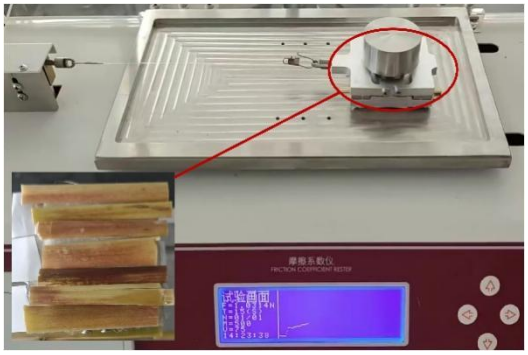

Fig. 4 - Friction coefficient measurement

Table 2

Measurement results of the friction coefficient of silage corn straw

Straw section	Coefficient of kinetic friction	Static Friction Coefficient
Straw epidermis—Steel	0.32±0.013	0.35±0.021
Straw core—Steel	0.58±0.053	0.62±0.057
Straw epidermis—Straw epidermis	0.09±0.004	0.11±0.016
Straw epidermis—Straw core	0.31±0.018	0.35±0.051
Straw core—Straw core	0.88±0.054	0.95±0.055

Mechanical Properties Testing of Straw

Straw Shear Testing

Corn stalks are rod-shaped with near-circular cross-sections, prone to rolling. To prevent specimen slippage and displacement during shear testing, a groove-type shear fixture was employed, as shown in Figure 5a. Three replicate shear tests were conducted at a sharing rate of 10 mm/min. The resulting shear force versus displacement curve is depicted in Figure 5b. As displacement increased, the shear force variation exhibited four distinct phases: rapid rise, abrupt decline, gradual increase, and gradual decline. These corresponded to the stages of compression failure, fiber rupture, and overall fracture during shearing. Due to the axial distribution of fibers along the stalk axis in silage corn stalks, the shear force curve displayed a sawtooth pattern.

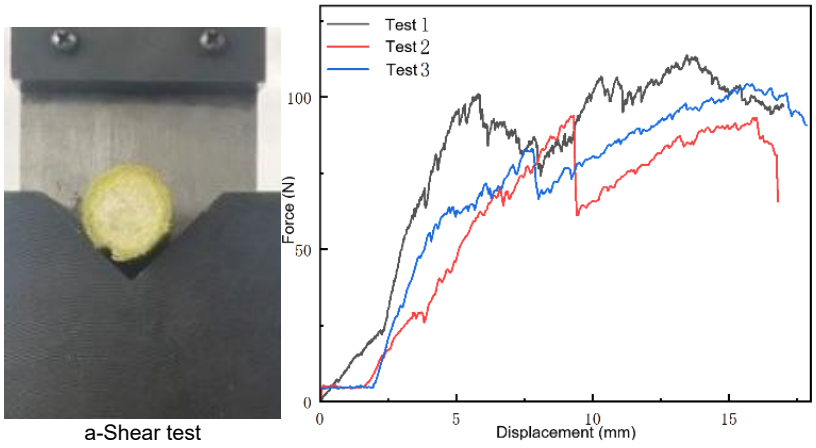

a-Shear test

b-Shear Test Load-Displacement Curve

Fig. 5 - Shear test

Three-Point Bending Test of Straw

As shown in Figure 6a, a universal testing machine was employed to conduct three-point bending tests with a gauge length of 60 mm. Loading was applied at a rate of 10 mm/min, with three replicate tests performed. The measured load-displacement curves are presented in Figure 6b. Silage corn straw exhibited linear elastic response within the 0–3 mm deflection range, with bending load rapidly increasing from 0 to 50–60 N. Beyond 3 mm deflection, the material entered the plastic stage. Microcracks initiated and propagated between fiber layers, causing fluctuations in the load curve and a significant deceleration in load increase.

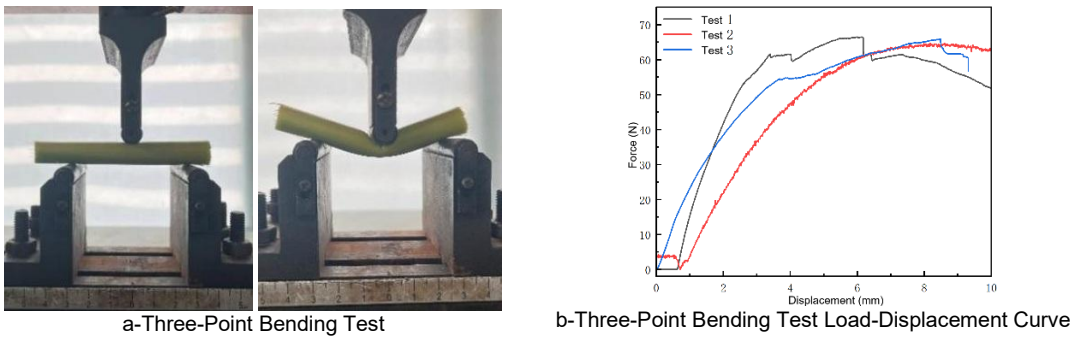

a-Three-Point Bending Test b-Three-Point Bending Test Load-Displacement Curve

Fig. 6 - Three-point bending test

Establishment of Discrete Element Models and Parameter Calibration

Development of the Straw Discrete Element Model

In this study, the Bonding V2 contact model within EDEM software was employed to accurately simulate the bonding interactions between corn stalk particles and their fracture behavior under external forces. This model generates virtual "bonding links" between discrete, adjacent particle pairs, introducing an additional constraint force that limits relative particle motion. This enables the particles to exhibit continuum behavior characteristic of solid materials (*Raji et al., 2004*). As shown in Figure 7, bonded particles are independent spheres that do not overlap and interact only at contact points. Bonding links form between particles when the distance between them falls within the contact radius.

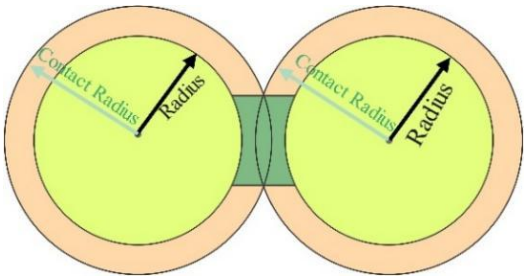

Fig. 7 - Bonding model

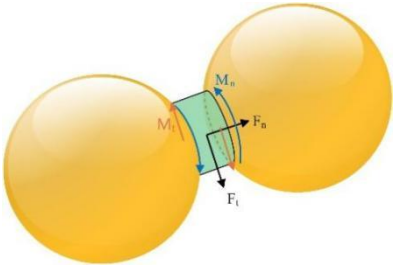

Fig. 8 - Stress analysis of the bonding key

The strength of an adhesive bond is primarily determined by four parameters: normal adhesive stiffness, tangential adhesive stiffness, normal strength, and shear strength. Among these, normal and tangential adhesive stiffness respectively govern the bond's resistance to normal and tangential deformation, while normal and tangential strength respectively define the ultimate stress at which the bond fractures in the normal and tangential directions, as shown in Figure 8.

The cohesive bonds between particles resist relative normal and tangential motion, with their failure conditions satisfying Equations (2) and (3):

$$\sigma_{\max} < -\frac{F_n}{A} + \frac{2M_t}{JRB} \quad (1)$$

$$\tau_{\max} < -\frac{F_t}{A} + \frac{M_n}{JRB} \quad (2)$$

where:

$\sigma_{\max}$ is the maximum normal stress, N/m²;

$\tau_{\max}$ is the maximum shear stress, N/m²;

F_n is the normal force, N;

F_t is the tangential force, N;

A is the contact area, m2;

M_t is the tangential torque, N·m;

M_n is the normal torque, N·m;

R is the particle radius, m;

B is the scaling factor for the bonding plate.

Corn stalks can be regarded as cylindrical structures regardless of whether segments are taken from the upper, middle, or lower sections. The upper internodes of silage corn stalks are slender and have low strength, making them prone to bending under compression rather than shear failure; simulation results are sensitive to parameter perturbations. The lower internodes are short and thick, exhibiting complex surface cutting behavior that fails to represent the main stalk structure. The middle internodes possess moderate length and diameter, with a vascular bundle-to-parenchyma cell ratio close to the plant-wide average. Therefore, this study employs the middle section for simulation. To balance computational efficiency and accuracy, the particle radius is set to 0.43 mm and the contact radius to 0.6 mm. Considering the complex physical and biological microstructure of corn stalks, they are simplified into isotropic bulk elements for systematic analysis of macroscopic mechanical properties. Based on a hexagonal close-packed (HCP) arrangement, a discrete element model of corn stover with regular particle distribution was generated, featuring a length of 20 mm and a diameter of 15 mm. As shown in Figure 9, this model comprises 4,235 particles, generating a total of 18,980 cohesive bonds.

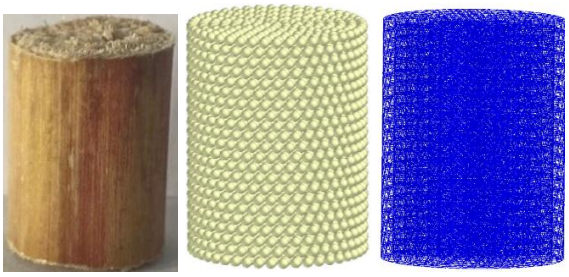

Fig. 9 - Corn stalk and corresponding simulation model

Discrete Element Simulation Analysis

Simulation of Corn Stalk Shearing Process

After establishing the discrete element model of corn stalks, a discrete element simulation of the shearing process was conducted, as shown in Figure 10. The motion parameters of the shearing tool were set to enable gradual contact between the tool and the stalk until radial shear failure of the stalk was achieved.

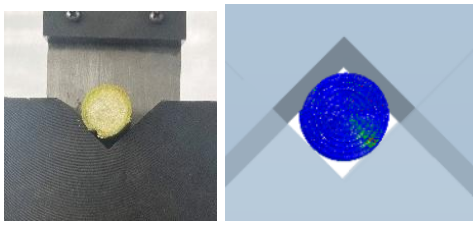

Fig. 10 - Discrete element simulation of shear process

As the displacement of the shear tool increases, the fracture process of cohesive bonds between stem particles evolves as shown in Figure 11. At the onset of shearing (Figure 11a), the internal cohesive bonds within the specimen are uniformly distributed in a complete grid-like pattern with no fracture zones, maintaining a stable and continuous structural connection. As shearing progresses (Figure 11b), the cohesive bonds gradually rupture, causing deformation and damage to the network structure. This leads to significant separation deformation of the specimen along the shear direction, ultimately forming a distinct shear failure morphology (Figure 11c).

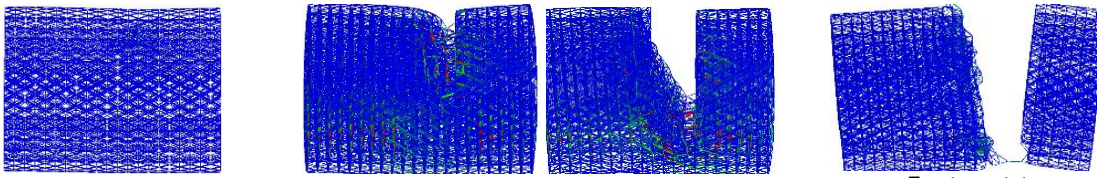

Fig. 11 - Simulation results of the shearing process

Parameter Sensitivity Analysis

To ensure simulation accuracy and achieve an optimal balance between computational efficiency and simulation precision, this study conducted sensitivity analyses on two key parameters: time step and loading rate. The time step setting directly impacts numerical stability and computational efficiency, while the loading

rate influences the simulation quality of the quasi-static process and the dynamic response of the granular system. A random set of parameter combinations (detailed in Section 2.3.1) was selected. Using the control variable method, the shear force response of straw was investigated at loading speeds of 7.5 mm/s, 10 mm/s, and 15 mm/s, and time steps of 5%, 10%, 15%, and 20%. The experimental design is shown in Table 3.

Table 3

Sensitivity analysis test design		
Serial Number	**Shear loading speed**	**Time step**
1	10 mm/s	5%
2	5 mm/s	10%
3	7.5 mm/s	10%
4	10 mm/s	10%
5	15 mm/s	10%
6	10 mm/s	15%
7	10 mm/s	20%

Figure 12 illustrates the effects of tool loading speed and time step size on shear force. Using the shear force-displacement curve at a 5% time step as the baseline, when the time step increases to 10%, the peak shear force deviation is 0.02%. The simulated shear force-displacement curves remain largely consistent, demonstrating excellent agreement and convergence. However, when the time step increased to 15% and 20%, the peak shear force deviation rose to 14.08% and 26.32%, respectively. The peak shear intensity decreased, and the simulation results showed significant deviations. At the same time, numerical fluctuations intensified, indicating that numerical stability had significantly deteriorated and no longer met accuracy requirements. Therefore, balancing computational efficiency and numerical stability, a 10% time step was ultimately selected as the standard time step for subsequent simulations. Using the shear force-displacement curve at a loading speed of 5 mm/s as the baseline, at the same displacement. At a velocity of 10 mm/s, the maximum deviation of the shear force-displacement curve was 26.07%, with a peak deviation of 7.43%; at 15 mm/s, the maximum deviation was 20.69%, with a peak deviation of 1.26%. However, at a loading speed of 15 mm/s, the shear force-displacement mechanical response exhibited significant divergence. The timing difference in reaching the ultimate stress process was large, with a peak lag of up to 8 mm. At this loading speed, the system's mechanical response deviated from the quasi-static assumption, and the interference from inertial effects could not be ignored. This compromised the accuracy and reliability of the simulation results. Therefore, the 15 mm/s loading speed is unsuitable for the simulation analysis in this study. Given the substantial computational demands of the discrete element method simulation, a loading speed of 10 mm/s is selected as the standard to achieve a reasonable balance between efficiency and accuracy while ensuring the precision and reliability of the results.

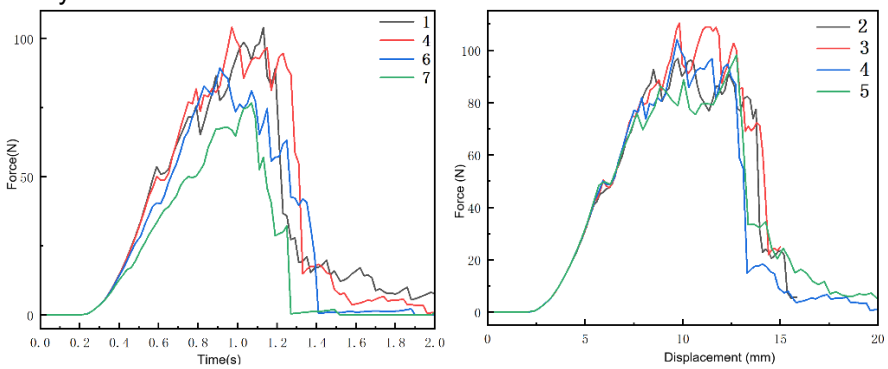

Fig. 12 - Sensitivity analysis simulation results

Calibration of the Discrete Element Model for Corn Stalks

Determination of Parameter Ranges

To systematically investigate the impact of multi-parameter coupling effects on simulation results within the stalk particle discrete element model, this study employs Latin Hypercube Sampling (LHS) to generate samples within a predefined parameter space. LHS is a stratified random sampling technique that achieves higher spatial coverage and convergence efficiency with the same sample size, making it particularly suitable for parameter exploration in high-dimensional, nonlinear systems. Initial parameter ranges were first determined through a literature review, as shown in Table 4.

Table 4

Range of bonding parameters		
Parameter Name	lower limit	upper limit
P1	1×10^{9}	1×10^{11}
P2	1×10^{8}	1×10^{10}
P3	1×10^{7}	1×10^{9}
P4	1×10^{6}	1×10^{8}

Simulation analysis was conducted on the range parameters in Table 4, with the result distribution shown in Figure 13. The yellow region represents the spatial domain of the simulation results. It can be observed that the experimental results fall within the simulated range, and the minimum and maximum values of the numerical simulation are comparable to the experimental reference values. Therefore, this range can serve as the parameter range for subsequent calibration.

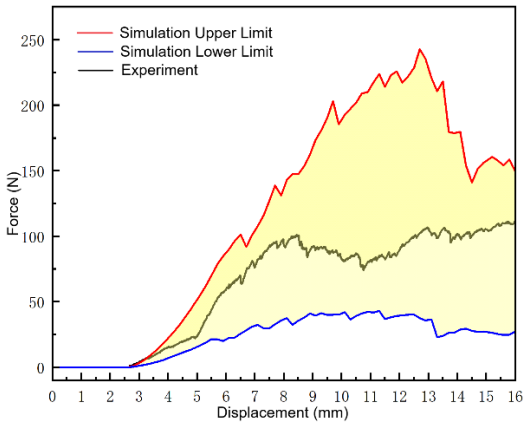

Fig. 13 - Distribution range of simulation results

Utilize Latin hypercube sampling to partition each parameter's defined range probabilistically and randomly draw samples, ensuring only one sample is drawn from each subinterval.

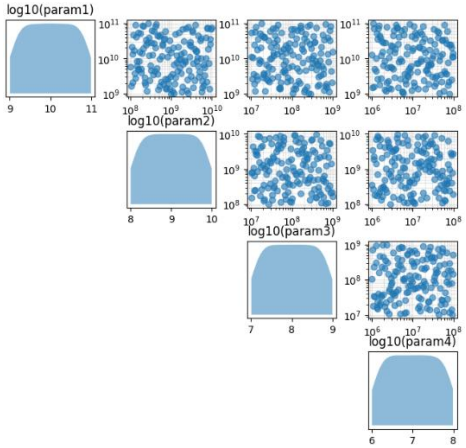

Fig. 14 - Parameter sample distribution

As shown in Figure 14, the Latin hypercube sampling results ensure both uniform coverage of values in single-parameter dimensions and spatial representativeness across multiple-parameter dimensions. This provides reliable sample support for subsequent tasks such as model response analysis and parameter sensitivity assessment.

Bayesian Optimization

Bayesian optimization is an adaptive hyperparameter optimization method based on sequential global optimization strategies (*Chen et al., 2025*). It is well-suited for scenarios where objective function computation is costly and involves black-box functions, making it ideal for DEM parameter calibration.

This study employs a Gaussian process regression as the surrogate model within the Bayesian optimization framework to approximate the mathematical relationship between micro-parameters and macro-responses, with the objective function defined as the acquisition function.

Mean squared error (MSE) is selected as the quantitative metric to assess the fit between experimental data and simulation results. Using linear interpolation, 1000 uniformly distributed displacement points were generated within the common displacement range. Stress values at these points were calculated by connecting adjacent data points. As a common error assessment metric, MSE accurately reflects the deviation between simulated predictions and experimental data. A low MSE value indicates minimal error between simulation results and actual experimental data. Its calculation formula is:

$$\mathrm{MSE}=\frac{1}{\mathrm{n}}\sum_{i=1}^{n}(y_i-\hat{y}_i)^2 \tag{3}$$

where:

y_i is the experimental actual value;

$\hat{y}_i$ is the simulation predicted value.

As shown in Figure 15, Bayesian optimization constructs a Gaussian process based on existing experimental results and trains it using 150 sets of DEM simulation sample points. Based on the current surrogate model's prediction and exploration of the objective function, a balanced strategy selects the most promising parameter combinations within the parameter space for evaluation. The obtained optimal parameter combinations are then applied to actual DEM simulations to derive new objective function values. As optimization progresses, the surrogate model gradually improves, enabling more precise guidance for parameter space exploration. After 100 iterations, the parameter combination yielding simulation results closest to experimental data is identified, thereby completing the parameter calibration optimization process.

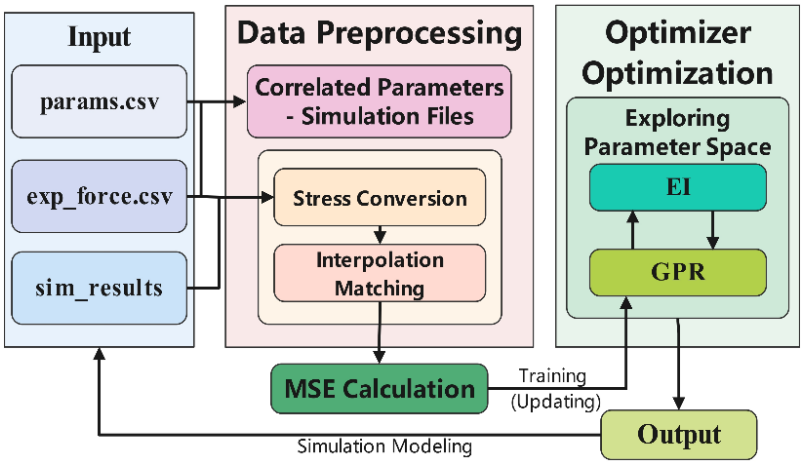

Fig. 15 - Bayesian optimization flow chart

RESULTS

Bayesian Optimization Results

Figure 16 illustrates the predicted MSE variation over 100 iterative cycles. During the initial 40 iterations, the model's predicted MSE exhibited significant fluctuations with consistently high values, indicating substantial influence of parameter combinations on prediction accuracy and insufficient spatial exploration. After 40 iterations, the model's predicted MSE exhibited an overall downward trend, stabilizing between 0 and 0.025 without significant variation. This indicates the optimization algorithm had identified a parameter combination approaching the global optimum. Following 100 iterations, the model's predicted MSE reached 0.0072.

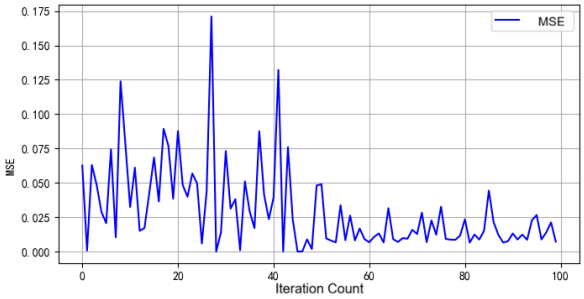

Fig. 16 - MSE convergence curve

The optimal parameter combinations are shown in Table 5.

Table 5

Bayesian optimization results	
Parameter	Parameter value
P1	5.12×10^{9}
P2	1.28×10^{8}
P3	1.60×10^{7}
P4	2.48×10^{6}

To validate the reliability of the aforementioned optimal parameter combination, a shear simulation was conducted on the discrete element model of silage corn stalks, comparing the agreement between the simulated and experimental stress-strain curves. As shown in Figure 17, the simulated curve closely matches the experimental curve in both shape and fluctuation amplitude. Calculations reveal that the Mean Squared Error (MSE) between the simulated and experimental stress-strain curves is 0.0034. This indicates that the simulation model, based on the optimized parameter combination, effectively captures the variation patterns observed in the experimental data and accurately reflects real-world conditions.

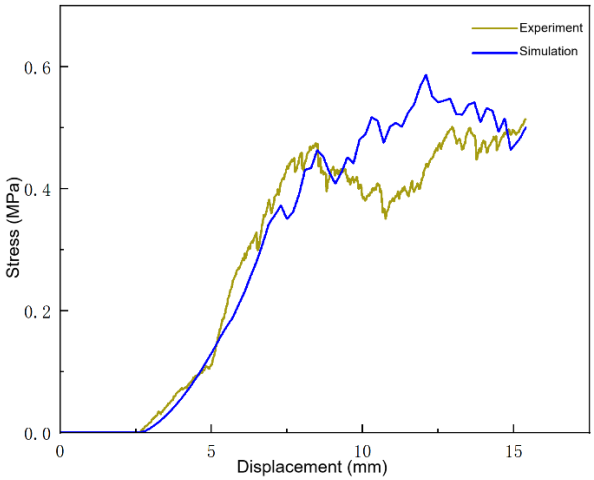

Fig. 17 - Comparison of the straw shear test and simulation test results

Parameter Sensitivity Analysis

Figures 18 and 19 illustrate the impact of the P1-P2 and P3-P4 interactions on MSE, respectively. The figures reveal that MSE exhibits distinct nonlinear characteristics with parameter variations, indicating high sensitivity of model outputs to individual parameters and strong interaction effects between parameters. In Figure 18, the MSE reaches its minimum when P1 is at an intermediate level, indicating that the model predictions are closest to the experimental results at this point. As P2 increases, the MSE shows little change, suggesting that P2 has a minor influence on the MSE.

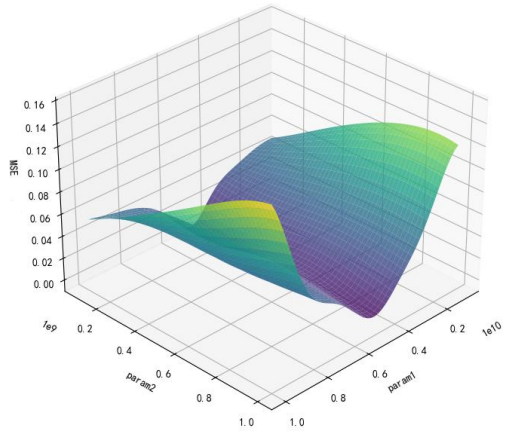

Fig. 18 - P1 and P2 interaction diagram

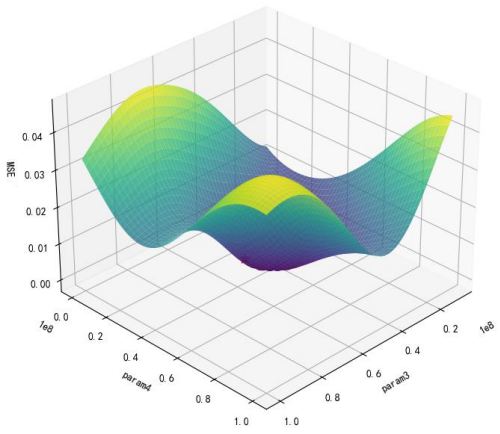

Fig. 19 - P3 and P4 interaction diagram

Figure 19 illustrates the interactive effect of P3 and P4 on MSE. It can be observed that under the influence of these two parameters, the MSE curve exhibits a distinct “concave valley” shape within the parameter space. Both parameters exert a significant impact on MSE, with the optimal parameter combination occurring at the deepest point of the valley.

Model Validation

To further validate the accuracy of the calibrated parameter combination, a three-point bending simulation was conducted, as shown in Figure 20.

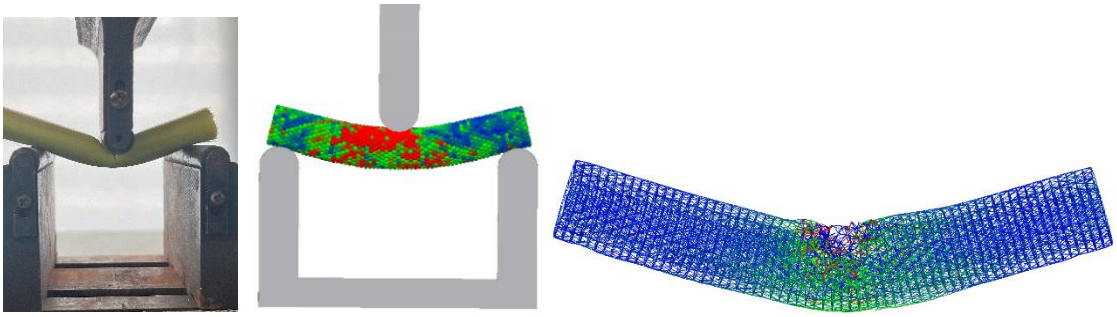

Fig. 20 - Numerical simulation of three-point bending of straw

As shown in Figure 21, both experimental and simulated stress-strain curves exhibit an overall trend of rapid initial increase followed by a decline. Experimental data show a steeper stress rise, while simulated data exhibit a relatively gentler ascent with delayed peak occurrence. The MSE between the two sets of data is 0.0159, attributed to significant mechanical property differences between the straw epidermis and inner pith. The peak deviation between experimental and simulated results is 0.06%. Therefore, the calibrated parameters are considered to adequately represent the overall mechanical properties of the straw.

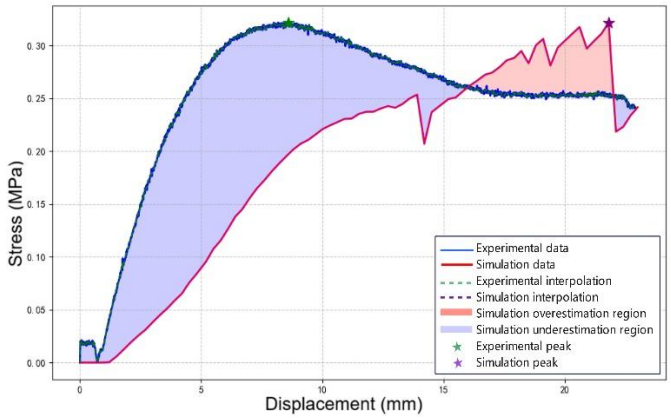

Fig. 21 - Comparison of the straw three-point bending test and simulation test results

CONCLUSIONS

This study employed Bayesian optimization to calibrate four bonding parameters, yielding optimal parameter combinations. Validation analysis against experimental data led to the following key conclusions:

(1) By calibrating the four bonding parameters using Bayesian optimization with MSE as the objective function, 100 iterations yielded a predicted MSE of 0.0072. This process identified an optimal parameter combination that significantly enhances simulation accuracy: Normal bond stiffness, tangential bond stiffness, normal strength, and shear strength were determined to be 5.12×10^{9} N/m³, 1.28×10^{8} N/m³, 1.60×10^{7} Pa, and 2.48×10^{6} Pa, respectively.

(2) Stress-strain curves from shear and three-point bending tests were compared with simulation results. The MSE between the shear test and simulation stress-strain curves was 0.0034. Both the overall trend and critical points of the three-point bending test results showed high consistency with simulations. This validated that the optimized simulation model can effectively predict the mechanical behavior observed in actual experiments.

(3) Due to significant differences in mechanical properties between the husk and pulp of silage corn stalks, a single homogeneous model proved suboptimal during parameter optimization validation. Future research may develop a “husk–pulp” dual-layer discrete element structure. By assigning distinct parameters and calibrating independently for each layer, precise characterization of mechanical behavior can be achieved, thereby enhancing simulation reliability and equipment design accuracy.

ACKNOWLEDGEMENT

This work was supported by the following projects:

Shandong Provincial Natural Science Foundation - Youth Fund. Project No.: ZR2024QE132

Shandong Provincial Pilot Project for Integrated R&D, Manufacturing, and Application of Agricultural Machinery: R&D, Manufacturing, and Application of Intelligent Silage Harvesters. Project Number: NJYTHSD-202312

National Key R&D Program Project: Development and Application of Intelligent Technology and Equipment for Quality-Preserving Harvesting of High-Quality Silage Forage. Project Number: 2022YFD2001905

Shandong Provincial Pilot Project for Integrated R&D, Manufacturing, and Application of Agricultural Machinery: R&D, Manufacturing, and Application of Intelligent Harvesting Equipment for Woody Forage Crops. Project No.: NJYTHSD-202316

REFERENCES

[1] Chen, C., Luo, W., Tang, S., Jia, Z., Sun, S., Zhang, Z., Zhu, W., (2018). Drainage layout in paddy fields meeting machinery harvest requirement based on DRAINMOD mode (满足机械收割农艺条件下稻田排水暗管布局 DRAINMOD 模型模拟). *Transactions of the Chinese Society of Agricultural Engineering*, Vol.34(14), pp. 86-93, Beijing/China.

[2] Chen, W., Liu, C., Fan, B., Feng, Q., Ding, J., He, W., (2025). Prediction of bran speck content in wheat flour based on XGBoost with Bayesian optimization (基于贝叶斯优化 XGBoost 的小麦粉麸星含量预测). *Journal of Henan University of Technology (Natural Science Edition)*, Vol. 46(01), pp. 105-113, Henan/China.

[3] Cundall, P. A., Strack, O. D. L., (1979). A discrete numerical model for granular assemblies. *Géotechnique*, Vol. 29(1), pp.47-65, England.

[4] Du, Z., Li, D., Li, X., Jin, X., Wu, Y., Yu, F., (2025). Calibration and Experiment of Discrete Element Model Parameters for Tea Stem (茶茎秆离散元模型参数标定与试验). *Transactions of the Chinese Society for Agricultural Machinery*, Vol. 56(01), pp. 311-320, Beijing/China.

[5] Fandi, Z., Diao, H., Liu, Y., Ji, D., Dou, M., Cui, J., Zhao, Z., (2024). Calibration and Validation of Simulation Parameters for Maize Straw Based on Discrete Element Method and Genetic Algorithm–Backpropagation. *Sensors*, Vol. 24(16), pp. 5217-5217, Switzerland.

[6] Fu, H., Wu, Z., Duan, J., Yu, S., Liu, F., Zheng, H., (2025). Calibration of contact parameters of ‘Luli’ apple for simulation based on discrete element (基于离散元的‘鲁丽’苹果仿真接触参数标定). *Journal of South China Agricultural University*, Vol. 46(03), pp. 407-418, Guangdong/China.

[7] Guan, Z., Mu, S., Li, H., Jiang, T., Zhang, M., Wu, C., (2022). Flexible DEM Model Development and Parameter Calibration for Rape Stem. *Applied Sciences*, Vol. 12(17), pp. 8394-8394, United Kingdom.

[8] Gun, H., Han, J., Lv, Z., Dong, Y., Guo, L., Zhou, W., (2025). Discrete Element Model Construction and Parameter Calibration of Combined Harvest Oil Sunflower Extract (联合收获油葵脱出物离散元模型构建与参数标定). *Transactions of the Chinese Society for Agricultural Machinery*, Vol. 56(05), pp.319-330, Beijing/China.

[9] Guo, X., Cui, W., (2002). Research Progress on Enhancing the Utilization Rate and Nutritional Value of Straw Feed (提高秸秆饲料利用率和营养价值的研究进展). *Feed Industry*, (11), pp.12-15, Liaoning/China.

[10] He, D., Li, H., He, J., Lu, C., Wang, C., Wang, Y., Wu, Z., Tong, Z., Gao, Z., (2025). Research on vibration characteristics of no-tillage seeding unit based on the MBD-DEM coupling. *Computers and Electronics in Agriculture*, Vol. 230, pp. 109877-109877, Netherlands.

[11] Hou, X., Zhang. X., Xu, J., Xu, P., Huang, S., Shen, J., Zhang, C., (2023). Evaluating the energy efficiency of tractors under actual operating conditions (基于实际作业工况的拖拉机能效评价). *Transactions of the Chinese Society of Agricultural Engineering*, Vol. 39(21), pp. 29-35, Beijing/China.

[12] Li, H., Meng, Y., Qi, X., Wang, Y., Li, Y., Li, M., (2025). Discrete Element Modelling Method and Parameter Calibration of Garlic Species Based on Bonding V2 Model (基于 Bonding V2 模型的蒜种离散元建模与参数标定). *Transactions of the Chinese Society for Agricultural Machinery*, Vol. 56(07), pp.150-157+169, Beijing/China.

[13] Liang, S., Liu, L., Liu, F., Chang, H., Cui, W., Li, G., (2025). Establishment and calibration experiment of the discrete element model for spinach root-soil complex (菠菜根土复合体离散元模型建立与标定试验). *Transactions of the Chinese Society for Agricultural Machinery*, Vol. 41(05), pp. 38-49, Beijing/China.

[14] Liu, F., Zhang, J., Chen, J. (2018). Modeling of flexible wheat straw by discrete element method and its parameters calibration. International *Journal of Agricultural and Biological Engineering*, Vol. 11(3), pp. 42-46, Beijing/China.

[15] Liu, Q., Sun, Q., Xu, l., Yang, W., Qiao, X., Liu, X., (2018). Effects of Chopping and Shredding on the Silage Quality of Corn Stalk (切碎和揉丝对玉米秸秆青贮品质的影响). *China Dairy Cattle*, (05), pp. 7-10, Beijing/China.

[16] Liu, W., Su, Q., Fang, M., Zhang, J., Zhang, W., Yu, Z., (2023). Parameters Calibration of Discrete Element Model for Corn Straw Cutting Based on Hertz-Mindlin with Bonding. *Applied Sciences*, Vol. 13(2), pp. 1156, Switzerland.

[17] Liu, Y., (2023). Simulation and Experimental Study of Corn Stalk Shredding Based on the Discrete Element Method (基于离散元法的玉米秸秆揉丝仿真与试验研究). *Gansu Agricultural University*, Gansu/China.

[18] Lu, X., (2021). Analysis of China's Forage Crop Production in 2020 and Outlook for 2021 (2020 我国饲草商品生产形势分析与 2021 年展望). *Animal Agriculture*, (03), pp. 31-36, Beijing/China.

[19] Ma, Y., Wang, Z., Shi, L., Zhao, W., Sun, B., Dai, F., Li, H., (2025). Determination the intrinsic parameters and calibration of contact parameters for wheat seed particles (冬小麦种子颗粒离散元仿真参数标定). *Journal of China Agricultural University*, Vol. 30(03), pp. 175-184, Beijing/China.

[20] Raji A.O., FJ, Favier F., (2004). Discrete element modelling of the compressive loading of bulk agricultural particulates: Parametric studies. *Journal of Modeling, Design and Management of Engineering Systems*, Vol. 2(1), Nigeria.

[21] Shentu, J., Lin, B., (2023). A novel machine learning framework for efficient calibration of complex DEM model: A case study of a conglomerate sample. *Engineering Fracture Mechanics*, Vol. 279.

[22] Wang, W., Li, X., (2005). A Review on Fundamentals of Distinct Element Method and Its Application in Geotechnical Engineering (离散元法及其在岩土工程中的应用综述). *Geotechnical Engineering Technique*, Vol. 19(04), pp. 177-181, Beijing/China.

[23] Xie, L., Huang, J., Yin, C., Zhang, S., Jing, L., Jiang, Z., (2025). Measurement of Physical Parameters and Calibration of Discrete Element Simulation Parameters for 'Cui Bi No. 1' Tobacco Seeds ('翠碧一号'烟草种子物性参数测量与离散元仿真参数标定). *Journal of Fujian Agriculture and Forestry University (Natural Science Edition)*, pp. 1-12, Fujian/China.

[24] Xing, F., (2017). Experimental Study on the Physical and Mechanical Characteristics of Corn Stover (玉米秸秆物理机械特性试验研究). *Shenyang Agricultural University,* Liaoning/China.

[25] Xu, T., Yu, H., Huang, D., Yu, Y., Li, C., Gou, Y., Wang, J., (2025). Modeling of olive fruit based on discrete element method and analysis of the sensitivity of Young's modulus parameters (基于离散元法的油橄榄果实建模及杨氏模量参数灵敏度的分析). *Transactions of the Chinese Society of Agricultural*

Engineering, Vol. 41(09), pp. 175-182, Beijing/China.

[26] Yu, J., Fu, H., Li, H., Shen, Y., (2005). Application of discrete element method to research and design of working parts of agricultural machines (离散元法及其在农业机械工作部件研究与设计中的应用). *Transactions of the Chinese Society of Agricultural Engineering*, Vol. 21(05), pp. 1-6, Beijing/China.

[27] Zhang, G., Chen, L., Liu, H., Dong, Z., Zhang, Q., Zhou, Y., (2022). Calibration and experiments of the discrete element simulation parameters for water chestnut (荸荠离散元仿真参数标定与试验). *Transactions of the Chinese Society of Agricultural Engineering*, Vol. 38(11), pp. 41-50, Beijing/China.

[28] Zhao, H., Wang, X., Zheng, Z., Li, X., Huang, Y., (2025). Research Status and Progress of Discrete Element Method Applications in Agricultural Equipment (农业装备领域离散元法应用研究进展). *Transactions of the Chinese Society for Agricultural Machinery*, Vol. 56(07), pp. 1-19, Beijing/China.